frontiers | Frontiers in Physics

TYPE Brief Research Report
PUBLISHED 01 September 2022
DOI 10.3389/fphy.2022.920687

OPEN ACCESS

EDITED BY
J. Mark Meacham,
Washington University in St. Louis,
United States

REVIEWED BY
Hui Chen,
Ningbo University, China
Mingyang Cui,
Massachusetts Institute of Technology,
United States

*CORRESPONDENCE
Itziar González,
iciar.gonzalez@csic.es

SPECIALTY SECTION
This article was submitted to Physical Acoustics and Ultrasonics, a section of the journal Frontiers in Physics

RECEIVED 14 April 2022
ACCEPTED 28 July 2022
PUBLISHED 01 September 2022

CITATION
Luzuriaga J, Carreras P, Candil M, Bazou D and González I (2022), Acoustophoretic particle manipulation in hybrid solid/gel resonators. *Front. Phys.* 10:920687. doi: 10.3389/fphy.2022.920687

Acoustophoretic particle manipulation in hybrid solid/gel resonators

Jon Luzuriaga[1], Pilar Carreras[2], Manuel Candil[3], Despina Bazou[4] and Itziar González[3]*

[1]Signaling Lab, Department of Cell Biology and Histology, Faculty of Medicine and Nursing, University of the Basque Country (UPV/EHU), Leioa, Spain, [2]Department of Hematology, Hospital Universitario Doce de Octubre, Madrid, Spain, [3]ITEFI, Group of Ultrasonic Resonators RESULT, Spanish National Research Council CSIC, Madrid, Spain, [4]Department of Hematology, Mater Misericordiae University Hospital, Dublin, Ireland

This study presents a proof of concept to demonstrate the ability of ultrasounds to perform acoustophoretic processes in hybrid millifluidic resonators that include channels laterally embedded in extremely soft media with physical properties close to those of liquids. In our experiments, particles are driven by acoustic radiation forces toward hydrodynamic/acoustic equilibrium positions in a similar way to that produced in conventional microfluidic resonators with solid structures; 20 um-sized polystyrene beads immersed in deionized water flow channelized throughout an aqueous-based gel between an inlet and outlet in a resonant chamber while being exposed to ultrasounds at a frequency of 1.54 MHz. The liquid channel formed presents irregular walls and variable geometry defined by the sample injection pressure. Particles collect rapidly along a central line equidistant from the walls, regardless of whether they are parallel or not, as observed for different channel geometries and cross-sectional dimensions. Only when the flow stops, the particles collect in acoustic pressure nodes established with the 2D spatial distribution. These results break the paradigm of solid structures as essential physical elements to support acoustophoresis, demonstrating the ability to produce these processes in media without a consolidated structure. It opens a door to bioprinting applications.

KEYWORDS

free walls, ultrasonic resonators, liquid interface, particle manipulation, acoustofluidics

1 Introduction

Microfluidic devices offer advantages over conventional techniques by simplifying complex protocols commonly associated with them and reducing the size of the equipment required. Hundreds of millifluidic and microfluidic platform designs have been developed so far to carry out cell separation processes in laboratories, based on different governing mechanisms. They are highly efficient for various in-line sample handling applications for enrichment, separation, or modeling work, involving early

detection and monitoring techniques in liquid biopsy, environmental samples, and food engineering, among others. It is a current trend toward miniaturization and the combination of many biological processes from the laboratory to the micro-scale [1–7].

Different mechanisms are used as the working basis of lab-on-chip platforms, including the size of elements to be manipulated, and their shape, deformability, and density. Different working approaches are developed depending on the size of particles or cells [8–15], use spiral channelizations [16–19], channels with contraction/expansion reservoirs, micro-scale vortices [20, 21], micron-sized gaps [22], serpentine microfluidic channels, micropillars [23–26], or membrane microfilters [27], among others. Other properties, such as their electrical charge, and magnetic or migratory properties, are also considered. In particular, optical and electrophoretic manipulations of cells have been carried out extensively for several decades. Among these microfluidic or millifluidic platforms, various configurations have been designed to perform acoustophoretic manipulation driven by ultrasonic waves of different shapes and frequencies combined with microfluidics. They use acoustic forces to drive and collect target particles in clusters or chains that operate on the size, density, and compressibility of different cell populations [28–48], either isolated or combined with other fields. These devices operate with relatively low-intensity waves and frequencies similar to those of ultrasonic and frequencies similar to ultrasonic imaging, with little impact on viability when acting on cells (high biocompatibility) [49]. Acoustic technology has clinical advantages for cancer and other pathological processes—can be used for clinical early detection and monitoring of treatments in liquid biopsy, preventing invasiveness in patients, for plasma and blood cell separation [46, 50–52]. It can also be applied in environmental and agri-food applications, for early detection and sorting of unwanted microelements in water and waste, sorting of crop sprouts, *etc*.

Acoustophoresis in microfluidics/milifluidics can be performed based on bulk acoustic waves (BAW) or surface acoustic waves (SAW), but recent technological developments show that PAW (plate acoustic wave) devices are also efficient in cell separation [45]. BAW approaches base their performance on resonances that are established inside the treatment channel, which requires the establishment of a liquid-phase standing wave between the channel walls. They have strong geometrical constraints, requiring strict parallelism of the walls and rigid chip materials to achieve high reflectivity (silicon or glass are typically used for the chip structure in BAW devices). These devices have a high manufacturing cost and have little versatility in their performance for collecting cells at fixed positions defined by the relationship between the wavelength and the cross-sectional dimensions of the channel. Devices using SAW can operate as standing or nonstationary waves, and are more versatile than BAW as they have no restriction specifications for channel width or stiffness, allowing variable positions for particle collection defined by selecting the electrical displacements of their interdigital transducers (IDTs). However, they are severely restricted at low frequencies due to physical gap requirements between the electrodes of their TDIs as well as their widths, which are in the order of half a wavelength. The configuration of IDTs to operate at frequencies below 10 MHz requires very large dimensions of IDTs and much larger thicknesses of the piezoelectric substrate to avoid Lamb waves. The SAW isolator literature refers to operating frequencies above 9 MHz. They have a high manufacturing cost and require clear rooms for fabrication.

However, the basic mechanisms of acoustophoresis can be induced on other microfluidic platforms with 2D and 3D ultrasonic resonances of the entire chip structure containing the treatment channel. The authors of the current study have demonstrated the feasibility of polymeric materials as alternative materials [46, 53, 54] in efficient BAW ultrasonic separators that base their actuation on 3D resonances of the whole chip structure.

The ability to perform acoustophoresis on vibrating plate structures, PAW, a unique case of BAW models restricted to 2D structural plate-like vibrations set on very thin polymeric chips with a strategic surface-to-volume ratio, has also been demonstrated [46]. These flexible ultrasonic separators present advantages of each of BAW and SAW type devices but discard some of their respective disadvantages. PAW devices are a real alternative to conventional acoustophoretic devices as they feature simple geometric designs, are highly reliable, exhibit acoustic versatility, and allow structural materials with a wide range of physical and chemical properties to suit a specific application, including biocompatibility for bioapplications. In addition, they have economic advantages associated with their low manufacturing cost and are easy to fabricate and integrate with other on-chip components for future assembly configurations.

Previous literature studies report the handling of acoustic particles and cells in soft matter, such as droplets and gels [55–60]. However, there are no studies reporting acoustophoresis within channels made in these extremely soft media—in particular, liquid samples flowing through gels and exposed to ultrasound.

In the current study, we wanted to discover the limits of acoustophoretic device requirements beyond the boundary of solid chips to test the feasibility of manipulating particles in aqueous suspensions flowing in channeled paths through an irregular and extremely soft aqueous gel.

1.1 Working principle: acoustic particle collection by a radiation force

The principle of operation of acoustophoresis is based on the concept of radiation force, induced by a nonlinear interaction of

the incident wave and waves scattered by particles. This hydrodynamic force acoustically induced acts on every single particle with a size much smaller than the acoustic wavelength λ. In a one-dimensional standing wave, this axial force FR_{Ax} can be expressed as follows [61] (Gor'kov 1962):

$$FR_{Axial} = -\frac{\pi P_0^2 V_p \beta_0}{2\lambda}\phi(\rho,\beta)\sin(2kx), \quad (1)$$

where V_p is the particle volume; $\phi = \frac{5\rho_p - 2\rho_0}{2\rho_p + \rho_0} - \frac{\beta_p}{\beta_0}$ is the acoustic contrast factor; ρ_0 and ρ_p, and β_0 and β_p are the density and compressibility of the fluid and particle, respectively; and "x" is the distance from the particle to the nearest node of pressure in the standing wave. According to this equation, particles collect in locations separated by a half wavelength distance ($\lambda/2$). Sign ϕ indicates the motion of particles either toward nodes ($\phi > 0$) or to antinodes in the standing wave ($\phi < 0$).

In-plane cell motion acoustically induced by variations in the spatial pressure distribution within a node plane gives rise to a lateral radiation force that drives cells to collect in finite lateral locations together with viscous acoustic streaming entrainments. The acoustic radiation- and streaming-induced particle velocity is proportional to the acoustic frequency, the particle size, its acoustic contrast factor, and other parameters such as the kinematic viscosity [56]. At the frequency of 1–2 MHz, a lateral radiation force dominates on particles immersed in water with sizes from 10 µm up, whereas acoustic microstreaming becomes dominant on particles smaller and close to 1µm, on which inertial forces become much weaker than surface force platforms [62]. "Eckart" large-scale acoustic streaming is due to energy absorption in the fluid phase and drives cells out of desired position platforms. However, they are negligible in short pathlength trap chambers.

Several theoretical and experimental studies published during the last two decades present theoretical analyses and experimental verifications of the effects of radiation forcing in one-dimensional, 2D, and 3D chambers, assuming different chamber geometries and dimensions in these studies [55, 61–64]. Some of the theoretical studies of 3D standing waves have reported numerical solutions of the governing equations obtained using the COMSOL Multiphysics® finite element software and modelized using iterative methods in the numerical solutions of the equations of motion (fourth-order Runge–Kutta) [65]. In these chambers, the solid wall is not essential, but the boundary conditions must be well established for the generation of the standing wave in the case of the BAW acoustic waveform performance that requires the establishment of pressure nodes within the channel. In devices driven by surface acoustic waves, no requirement is necessary on the boundary conditions for the establishment of pressure nodes; only a suitable shift between the faced IDTs promotes the generation of pressure nodes at different locations inside the channel without the establishment of standing waves.

A recent study was performed by Vargas et al. in 2021 to address it [63]. It reported a theoretical prediction for the acoustic behavior of multiple particles in 3D standing waves in resonant chambers with both rigid and free walls has been recently performed. The authors assumed free walls along one direction (x-axis) and rigid walls in the other two transverse directions (along y- and z-axes) (Figure 1).

Vargas et al. derived an expression for 3D acoustic potential U_{ac} (x, y, z) established in this chamber actuated by a one-dimensional plane wave, assuming hybrid boundary conditions with freedom along the x-axis:

$$\begin{aligned} U_{ac}(x,y,z)) = U_0\Big[& 2f_1 \sin^2(k_x x)\cos^2(k_y y)\cos^2(k_z z) \\ & - \cos 2(k_y y) \\ & - 3f_2\frac{k_x^2}{k^2}\cos^2(k_x x)\cos^2(k_y y)\cos^2(k_z z) \\ & - 3f_2\frac{k_y^2}{k^2}\sin^2(k_x x)\sin^2(k_y y)\cos^2(k_z z) \\ & - 3f_2\frac{k_z^2}{k^2}\sin^2(k_x x)\cos^2(k_y y)\sin^2(k_z z)\Big]. \end{aligned} \quad (2)$$

A 3D acoustic radiation force is derived from this acoustic potential: $F_R = -\nabla U_{Ac}$:

$$\begin{aligned} F_R = & -2k_x\phi U_0 \sin(2k_x x)\Big[\frac{1}{4} + \frac{1}{4}\cos(2k_y y)\cos(2k_z z) + \Big\{\frac{1}{4} \\ & - \frac{\phi' k_z^2}{2k^2}\Big\}\cos(2k_y y) + \Big\{\frac{1}{4} - \frac{\phi' k_y^2}{2k^2}\Big\}\cos(2k_z z) - \frac{\phi'}{2k^2}\{k_y^2 + k_z^2\}\Big]\vec{i} \\ & + 2k_y\phi U_0 \sin(2k_y y)\Big[\frac{1}{4} - \frac{1}{4}\cos(2k_x x)\cos(2k_z z) - \Big\{\frac{1}{4} \\ & - \frac{\phi' k_z^2}{2k^2}\Big\}\cos(2k_x x) + \Big\{\frac{1}{4} - \frac{\phi' k_x^2}{2k^2}\Big\}\cos(2k_z z) - \frac{\phi'}{2k^2}\{k_x^2 + k_z^2\}\Big]\vec{j} \\ & + 2k_z\phi U_0 \sin(2k_z z)\Big[\frac{1}{4} - \frac{1}{4}\cos(2k_x x)\cos(2k_y y) - \Big\{\frac{1}{4} \\ & - \frac{\phi' k_y^2}{2k^2}\Big\}\cos(2k_x x) + \Big\{\frac{1}{4} - \frac{\phi' k_z^2}{2k^2}\Big\}\cos(2k_y y) - \frac{\phi'}{2k^2}\{k_x^2 + k_y^2\}\Big]\vec{k} \end{aligned} \quad (3)$$

where ϕ' is defined as $\phi' = \frac{1}{3f_1/3f_2+1}$ from dispersion coefficients f_1 and f_2: $f_1 = 1 - 1/\rho c^2$ and $f_2 = \frac{2(\rho-1)}{2\rho+1}$. In this equation, $\rho = \frac{\rho_p}{\rho_l}$ is the ratio of densities between particles and fluid, and c is the relationship of particles and liquid sound velocities. In this equation, c refers to the sound speed and ϕ' does not refer to the acoustic contrast factor of Eq. 2 described as ϕ, but it includes added terms and is defined by functions f_1 and f_2. The incident plane wave exerted into this hybrid 3D resonant chamber generates a complex 3D radiation force on every single particle associated with the complex spatial pressure patterns, as described in Eq. 3.

In a short pathlength chamber with z-direction ≈$\lambda/4$, this field reduces to a 2D standing wave with a spatial distribution of pressure nodes and antinodes limited to the x–y plane, simplifying Eqs 2,3 with term reduction. In this study, we

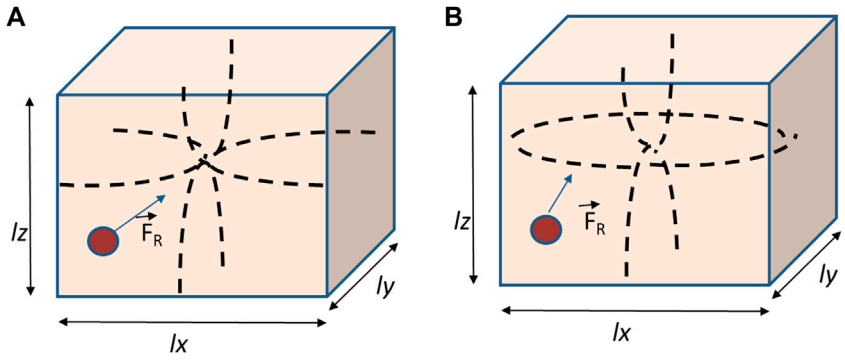

FIGURE 1
3D F_R acting on a spherical particle within a rectangular chamber of dimensions l_x, l_y, and l_z with a standing pressure field p_x (x), p_y (y), and p_z (z), respectively. **(A)** Chamber with all rigid walls; **(B)** rectangular chamber with free walls in x.

present a microfluidic hybrid resonant system combining rigid materials for the top and bottom of a circular chamber (quartz glass and aluminum, respectively) containing a coupling water-based gel crossed by a channel with flowing liquid samples. Thus, the channel acquires extremely soft lateral walls made up entirely of gel, that is, a channel with irregular, not parallel, viscous walls, with a variable geometry defined by the pressure of injection of samples. In this way, we investigate and demonstrate the feasibility of acoustophoretic manipulation of particles in straight and tortuous channels with irregular and extremely soft walls within unstructured media. Particle collection effects achieved in the experiments at a frequency of f = 1.54 MHz are similar to those achieved in conventional microfluidic platforms with solid structures actuated by ultrasounds.

2 Methods

2.1 Ultrasonic device

The device consists of a circular aluminum chamber with a diameter of 3 cm and a height of 0.5 mm actuated by an ultrasonic disk transducer (12 mm diameter) (Ferroperm, Kvistgard, Denmark) attached underneath and covered by a thin quartz-glass top reflector to allow microscopic imaging from above, as previously described in another research [42]. Figure 2A shows the schematic diagram of the setup. A transducer with a thickness resonance at a frequency close to 1.54 MHz was selected to perform the experiments as the drive frequency. The steel coupling layer on which the transducer was mounted had a thickness of $3\lambda_{steel}/4$. The chamber had an acoustic pathlength of one-half wavelength in water (0.5 mm) at the driving frequency and was covered by the quartz glass reflector with a thickness of 1 mm ($\lambda_{glass}/4$) to favor the establishment of a single pressure node plane located in the middle of the chamber height (Figure 2B). The "sample-containing" active area (inner diameter) of the cylindrical steel body had a diameter of 18 mm. The signal was supplied by a function generator (Agilent 33220A, Agilent Technologies Inc., Santa Clara, CA, United States). The thicknesses of different layers were selected to give a highly resonant system.

The chamber was filled with a hydrophilic water-soluble gel (ECG Parker aquasonic 100), which is extremely soft with a texture close to that of water, typically used in echography applications. An aqueous-based suspension of polystyrene micron-sized beads was injected by a syringe pump to flow through the gel between an inlet and an outlet located at diametrically opposite edges in the chamber. In this way, the flowing suspension opens channelization through the gel (Figure 3A). After removing the liquid sample from the device, its imprint remains as a hollow channel embedded in the gel volume (Figure 3B).

Samples consist of aqueous-based suspensions containing polystyrene 20 μm-sized beads in a concentration of approximately Cv~0.01% in deionized distilled water. These spherical particles present positive acoustic contrast factor ϕ to collect at the pressure nodes of the acoustic wave established in the area of the chamber occupied by the liquid phase.

2.1.1 Width and tortuosity of the liquid channel

The channel shape and width are defined by hydrodynamic parameters associated with the injection pressure and flow rate of the sample, which are in turn influenced by the particle concentration and physical properties of both, particles and liquid, as well as the texture of the surrounding gel (viscosity). According to them, it acquires paths with different geometry and tortuosity (Figures 3C,D). The lower the injection pressure, the slower the flow rate, which provide higher channel tortuosity due to higher resistance within the gel. This is associated with the viscous resistance of the gel to the opening of a channel by the suspension during its flow across it between the chamber inlet

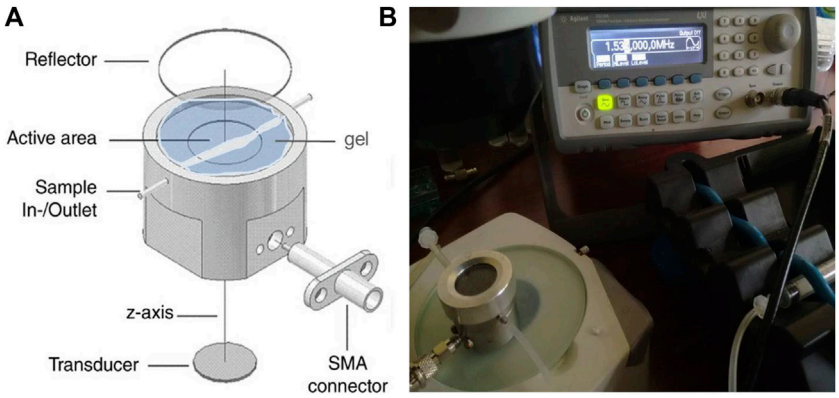

FIGURE 2
(A) Schematic diagram of the setup used to perform the acoustophoretic manipulation; **(B)** channelized path formed by the suspension flowing between the chamber inlet and outlet, surrounded by the aqueous-based gel.

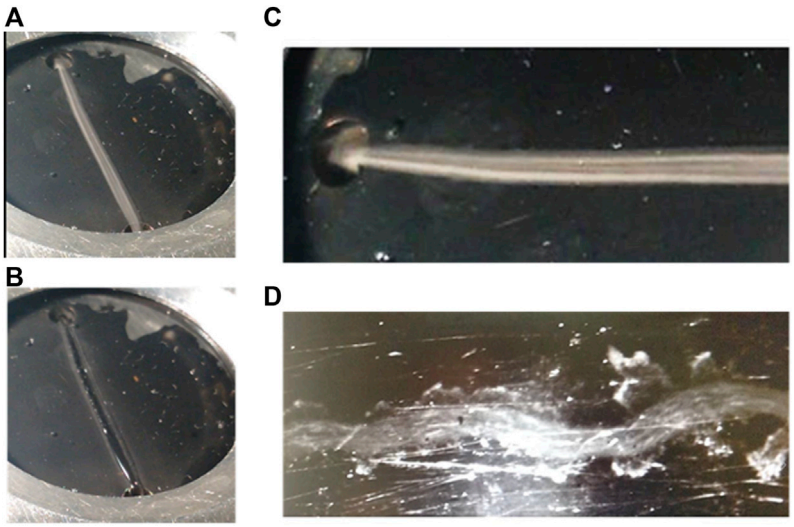

FIGURE 3
Aqueous-based suspension of polystyrene micron-sized beads; **(A)** flowing through a gel embedded in the resonating chamber; **(B)** channel imprint remaining as a hollow channel embedded in the gel volume after removing the suspension; **(C)** and **(D)** polystyrene-aqueous suspensions flowing at two different flow rates between the chamber inlet and outlet to draw "liquid channelizations" with different geometry and width throughout the gel matrix, which depends on the flow velocity of the sample, defined by the pressure of the injection.

and outlet. The lower the sample injection pressure, the weaker the force exerted by the liquid to flow through the gel, tracing a more tortuous and less straight channel, with irregular shape and width. On the contrary, higher flow rates generate thinner and straighter gel–liquid interfaces.

2.1.2 Estimation of the acoustic pressure amplitude (P_0)

The trap, driven at 1.54 MHz, had an acoustic pathlength of one-half wavelength in water (0.5 mm) at the driving frequency. P_0 was estimated previously by Bazou et al. (2005) in a study performed using this chamber of actuation whose volume was then entirely occupied by a water-based suspension instead of gel [66, 67]. This threshold pressure amplitude P_0 was determined from the voltage required to levitate a single 20 μm latex sphere in suspension against gravity by balancing the axial radiation force (in Eq. 1, for $z = \lambda/8$) with the buoyancy-corrected gravitational force. The pressure was demonstrated to be linearly proportional to the voltage applied to the

transducer at low supplied voltages. Thus, pressure amplitudes close to 0.05 MPa were obtained within the chamber at the frequency of f = 1.54 MHz and voltages around 5 $V_{P\text{-}P}$. In current experiments, approximately 70% of the chamber is filled with the water-based gel, with higher energy absorption than water. It means pressure amplitudes lower than 0.05 MPa were obtained in the chamber full of water.

2.1.3 Estimation of temperature increase during the ultrasonic actuation

Experiments were carried out for very short times of a few seconds. According to the previous study by Despina et al. performed with this chamber in 2005 [68, 69], an increase of temperature of less than 0.01K was reached at a pressure amplitude of 0.54 MPa for ultrasonic actuation of at least 30 min. In our current experiments, media impedances inside the chamber are also low and similar, at about Z = 1.6 in the parker aquasonic coupling gel and approximately Z = 1.5 MRayls in water [70]. However, heating effects of the ultrasound actuation on the sample temperature have been discarded in current experiments carried out for the very low supplied voltages and short times of actuation of few seconds, frequently ~1 s.

Poltawski et al. in 2008 [71] studied the transmission characteristics of a range of gel couplants using a radiation force balance. Ohlin et al. analyzed in 2015 [72] the relevance of the control of temperature in a resonant microfluidic device where they handled cells, whose viability had to be preserved. Recently, Cui et al. (2021) [73] analyzed thermal considerations for microswimmer trap and release using standing surface acoustic waves. They considered excessive heating due to vibration damping and other system losses potentially compromise the biocompatibility of the SAW technique with motile *Chlamydomonas reinhardtii* algae cells, also alive beings.

In the current work presented in this study, weak temperature variations below 1°C are not relevant for successful acoustophoresis results because it refers to experiments performed with polystyrene particles. In addition, our samples were flowing at high velocities varying from 2 mm/s up to 20 mm/s while being exposed to the ultrasonic actuation. The exposure of liquid samples to a flow motion prevents heating effects, following the same cooling principle typically applied with smart devices developed for outer space applications.

A microscopy imaging setup provided images with a spatial resolution of 10 μm per pixel. Thus, polystyrene 20-μm-diameter particles used in the experiments occupied 2 pixels ±1 pixel ~20 ± 10 μm in filmed images.

An estimate of the particle flow velocity before and during the ultrasonic actuation was achieved by using the PIV code of MATLAB and Image J freeware from consecutive filmed frames in each movie, resulting in $\overline{v_p}$ = 7 pixels/frame = 21 mm/s. Each particle crosses the entire channel length of 18 mm in somewhat less than 1 s in the case of straight channelization, but it requires longer time for channels with certain path tortuosity.

3 Results

Once the acoustic field is applied in the chamber, flowing particles rapidly collect along a line within the liquid phase as if a pressure node had been established on such a line centered between the liquid–gel interfaces, which act as the lateral channel walls.

The application of ultrasounds at the frequency of 1.54 MHz generates a 2D resonance in the chamber, including the gel and liquid sample within the channel. A radiation force is acoustically induced to act on particles, which were rapidly driven toward pressure nodes established in the standing wave, where they collect according to their positive acoustic contrast factor.

Figure 4A shows polystyrene beads filmed during their flow motion in deionized water before the ultrasound actuation, Figure 4B shows particles flowing while exposed to ultrasounds aligned along a central line in the channel, and Figure 4C shows particles collected in 2D pressure nodes when the sample is in rest and exposed to the ultrasonic wave.

Acoustic drift motion and collection effects were not expected on particles in the channel of our device because these acoustophoretic motions arise from the radiation force induced by ultrasounds and exerted on every single particle, directly related to the establishment of standing waves inside the channel. The impedance of the liquid medium in the channel and that of the gel are really similar (Table 1), and no wave reflection is expected at the interface between both media, required for the establishment of a standing wave. However, the experimental results have been different and show the feasibility of ultrasounds to collect particles along a central line in the channel regardless of the impedance relationship.

Both media differ mainly in their respective viscosities (this parameter defines a fluid's resistance to flow or an induced motion), with much higher magnitudes in gels than in water. However, viscosity is not a parameter involved in the acoustic impedance definition, $Z = \rho c$ (defined by density and sound speed), which defines the reflectivity of acoustic waves on the interface between the two media (channel walls).

Hence, the relevance of this experimental study that demonstrates the feasibility of acoustophoresis mainly based on a single parameter, viscosity. A certain difference in viscosity between the flowing liquid sample and the gel in the liquid–gel interface provides a certain consistency to channel walls and promotes a wave reflection to allow the particle collection inside the channel.

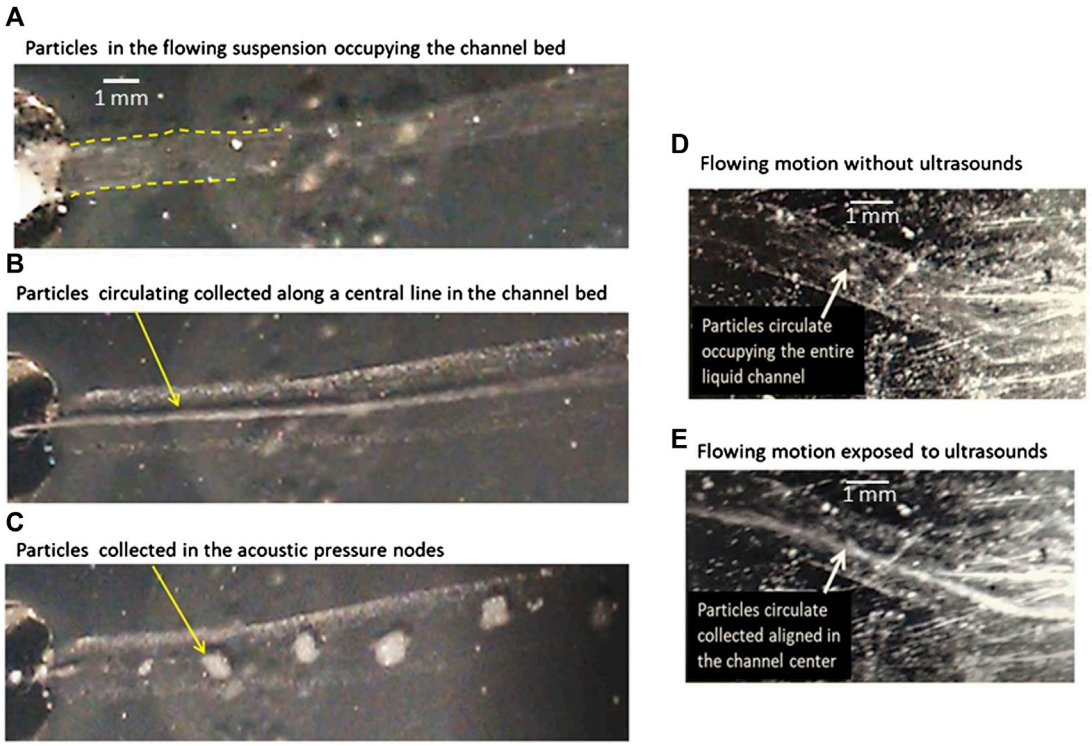

FIGURE 4
(A) Polystyrene beads of size 20 μm flowing in an aqueous suspension within a channel embedded in a gel without ultrasound exposure; **(B)** flowing at the same velocity and exposed to the acoustic wave at f = 1.54 MHz. The particles collect along a central line equidistant to the lateral gel–liquid interfaces; **(C)** collection of the particles exposed to ultrasounds in quiescent samples forming aggregates, without flow motion; **(D)** particles flowing homogeneously distributed within the channel path before their exposure to ultrasounds; **(E)** particle flow collected along a line once exposed to the ultrasonic wave.

TABLE 1 Properties of water and coupling aquasonic gel at room temperature of 20°C.

Medium	Density (g/c m^3)	Acoustic impedance, Z (MRayl)	Viscosity (cps)
Water	1.00	#202124; 1.48–1.50	#202124; 1
Aquasonic gel	1.02–1.03	~1.60	130.000–195.000

It must be remarked that this is a proof of concept, without quantitative analyses of the influence of flow rates or acoustic frequency on the effects of particle collection observed in the experiments. We also observed repeatedly that particles collected in a central line within the channel always in the midline between the walls, regardless of whether they were parallel, divergent, or convergent (Figures 4D,E). Despite the fact that the lateral limits of the channel are not exactly flat or parallel to each other and despite the shape of the channel, almost never straight, the acoustic collection of particles occurs in a few seconds once the acoustic field is applied.

These successful results obtained in more than 20 experiments performed at different flow velocities (varying from quiescent samples without moving up to 21 mm/s) show the need for a revision in the theoretical study of the radiation force in resonant chambers and, in particular, for chips without a solid structure, such as unconsolidated organic matter. Our findings point to the need for a revision in the theoretical definition of the axial and lateral expressions of the radiation force FR for resonant chambers with extremely soft but not free walls, which probably should include in its expression added terms referred to as the viscosities of both walls and liquid phase.

4 Conclusion

The study presented in this work is a proof of concept to analyze the limits in the physical property requirements of soft matter-based resonant devices for the manipulation of particles by acoustophoresis.

In this research, we experimentally demonstrate the ability of ultrasound to collect particles in microfluidic channels created in extremely soft media without a solid structure, beyond the concept of lab-on-chip. In particular, the concept of acoustophoresis can be extended to extremely soft media with a liquid phase flowing through aqueous-based gels with close density but different viscosity.

In these singular acoustophoretic assays, the parallelism between channel walls is not a key factor for the particle collection. However, the slight difference in viscosity and density between the gel and liquid phase allows to keep confined the liquid phase between lateral gel edges, behaving as partially reflective walls.

Regardless of the channel path, width, and geometrical shape, particles in flowing samples rapidly collect along a single central line established between lateral channel edges, where they continue their flow motion chained in the central line between the gel–liquid interfaces that act as pseudo-walls. The flow motion combined with strong spatial gradients of acoustic pressure amplitudes drives the particles toward a central position in the liquid phase. This is an unexpected behavior repeatedly observed in our 20 experiments.

We must emphasize that although the gel is a medium with an extremely smooth texture and properties very close to those of the liquid suspension, the particles' drift motion has been found similar to that of conventional microfluidic resonators with a solid structure surrounding the liquid phase flowing in the channel. These results break the paradigm of solid structures as essential physical elements to support acoustophoresis in channels based on the BAW actuation. This study confirms the ability of ultrasounds to handle particles in irregular channels embedded in extremely soft and unstructured media. It opens a door to future biomedical applications involving bio-printing procedures mimicking soft organic matter to handle flowing cells or particles in irrigation channelizations.

The results of this study open a door to a new technique that could be of interest in upcoming biomedical applications involving bioprinting procedures to handle flowing cells or particles in bioprinted mimicking samples that present channelization.

Data availability statement

The original contributions presented in the study are included in the article/Supplementary Materials; further inquiries can be directed to the corresponding author.

Author contributions

JL and PC have done equal contributions as first authors to the experimental research. MC has contributed to the work by participating in the experiments. DB has provided the trap device and knowledge from previous studies. IG led the work as an IP researcher.

Acknowledgments

This research was supported and funded by the National Research Project DPI2017-90147-R of Spain and by the National Research Council of Spain CSIC through project i-COOPA20348. The trap device belonging to Bazou was used for the experiments.

Conflict of interest

The authors declare that the research was conducted in the absence of any commercial or financial relationships that could be construed as a potential conflict of interest.

Publisher's note

References

1. Bhagat AAS, Bow H, Hou HW, Tan S, Han J, Lim CT. Microfluidics for cell separation. *Med Biol Eng Comput* (2010) 48:999–1014. doi:10.1007/s11517-010-0611-4

2. Bhardwaj P, Bagdi P, Sen AK. Microfluidic device based on a micro-hydrocyclone for particle–liquid separation. *Lab Chip* (2011) 11:4012–21. doi:10.1039/c1lc20606k

3. Tripathi S, Prabhakar A, Kumar N, Singh SG, Agrawal A. Blood plasma separation in elevated dimension T-shaped microchannel. *Biomed Microdevices* (2013) 15(3):415–25. doi:10.1007/s10544-013-9738-z

4. Sajeesh P, Sen AK. Particle separation and sorting in microfluidic devices: A review. *Microfluid Nanofluid* (2014) 17:1–52. doi:10.1007/s10404-013-1291-9

5. Nilghaz A, Shen W. Low-cost blood plasma separation method using salt functionalized paper. *RSC Adv* (2015) 5:53172–9. doi:10.1039/c5ra01468a

6. Tripathi S, Bala YV, Kumar V, Prabhakar A, Joshi SS, Agrawal A. Passive blood plasma separation at the microscale: A review of design principles and

microdevices. *J Micromech Microeng* (2015) 25:083001–0820024. doi:10.1088/0960-1317/25/8/083001

7. Xing X, He M, Qiu H, Yobas L. Continuous-flow electrokinetic-assisted plasmapheresis by using three-dimensional microelectrodes featuring sidewall undercuts. *Anal Chem* (2016) 88:5197–204. doi:10.1021/acs.analchem.6b00215

8. Di Carlo D. Inertial microfluidics. *Lab Chip* (2009) 9:3038–46. doi:10.1039/b912547g

9. Choi S, Song S, Choi C, Park J. Microfluidic self-sorting of mammalian cells to achieve cell cycle synchrony by hydrophoresis. *Anal Chem* (2009) 81:1964–8. doi:10.1021/ac8024575

10. Inglis DW. Efficient microfluidic particle separation arrays. *Appl Phys Lett* (2009) 94:013510. doi:10.1063/1.3068750

11. Tan SJ, Yobas L, Lee GYH, Ong CN, Lim CT. Microdevice for the isolation and enumeration of cancer cells from blood. *Biomed Microdevices* (2009) 11:883–92. doi:10.1007/s10544-009-9305-9

12. Hur SC, Mach AJ, Di Carlo D. High-throughput size-based rare cell enrichment using microscale vortices. *Biomicrofluidics* (2011) 5(2):0222061–10. doi:10.1063/1.3576780

13. Ma Y-MD, Wang L, Feng-Lei Yu PD. Recent advances and prospects in the isolation by size of epithelial tumor cells (ISET) methodology. *Technol Cancer Res Treat* (2013) 12(4):295–309. doi:10.7785/tcrt.2012.500328

14. Sollier. E, Go DE, Che. J, Gossett DR, O'Byrne. S, Weaver WM. Size-selective collection of circulating tumor cells using Vortex technology. *Lab Chip* (2014) 14(1):63–77.

15. Sheng W, Ogunwobi OO, Chen T, Zhang J, George TJ, Liu C, et al. Capture, release and culture of circulating tumor cells from pancreatic cancer patients using an enhanced mixing chip. *Lab Chip* (2014) 14(1):89–98. doi:10.1039/c3lc51017d

16. Gossett DR, Weaver WM, Mach AJ, Hur SC, Kwong Tse HT, Lee W, et al. Label-free cell separation and sorting in microfluidic systems. *Anal Bioanal Chem* (2010) 397:3249–67. doi:10.1007/s00216-010-3721-9

17. Hou HW, Warkiani ME, Khoo BL, Li ZR, Soo RA, Tan DS. Isolation and retrieval of circulating tumor cells using centrifugal forces. *Sci Rep* (2013) 3:1259. doi:10.1038/srep01259

18. Warkiani ME, Guan G, Luan KB, Lee WC, Bhagat AA, Chaudhuri PK. Slanted spiral microfluidics for the ultra-fast, label-free isolation of circulating tumor cells. *Lab Chip* (2014) 14(1):128–37. doi:10.1039/c3lc50617g

19. Khoo BL, Warkiani ME, Tan DS, Bhagat AA, Irwin D. Clinical validation of an ultra high-throughput spiral microfluidics for the detection and enrichment of viable circulating tumor cells. *PLoS One* (2014) 9(7):e99409. doi:10.1371/journal.pone.0099409

20. Stott SL, Hsu CH, Tsukrov DI, Yu M, Miyamoto D, Waltman BA, et al. Isolation of circulating tumor cells using a microvortex-generating herringbone-chip. *Proc Natl Acad Sci U S A* (2010) 107:18392–7. doi:10.1073/pnas.1012539107

21. Che J, Yu V, Dhar M, Renier C, Matsumoto M, Heirich K. Classification of large circulating tumor cells isolated with ultra-high throughput microfluidic Vortex technology. *Oncotarget* (2016) 7(11):12748–60. doi:10.18632/oncotarget.7220

22. Tan SJ, Lakshmi RL, Chen PF, Lim WT, Yobas L, Lim CT. Versatile label free biochip for the detection of circulating tumor cells from peripheral blood in cancer patients. *Biosens Bioelectron X* (2010) 26:1701–5. doi:10.1016/j.bios.2010.07.054

23. Nagrath S, Sequist LV, Maheswaran S, Bell DW, Irimia D, Ulkus L, et al. Isolation of rare circulating tumour cells in cancer patients by microchip technology. *Nature* (2007) 450(7173):1235–9. doi:10.1038/nature06385

24. Bhagat AAS, Hou HW, Li LD, Lim CT, Han J. Pinched flow coupled shear-modulated inertial microfluidics for high-throughput rare blood cell separation. *Lab Chip* (2011) 11:1870–8. doi:10.1039/c0lc00633e

25. Sarioglu F, Aceto N, Kojic N, Donaldson MC, Zeinali M, Hamza B. A microfluidic device for label-free, physical capture of circulating tumor cell clusters. *Nat Methods* (2015) 12(7):685–91. doi:10.1038/nmeth.3404

26. Kim B, Lee JK, Choi S. Continuous sorting and washing of cancer cells from blood cells by hydrophoresis. *Biochip J* (2016) 10(2):81–7. doi:10.1007/s13206-016-0201-0

27. Zheng S, Lin H, Liu JQ, Balic M, Datar R, Cote RJ, et al. Membrane microfilter device for selective capture, electrolysis and genomic analysis of human circulating tumor cells. *J Chromatogr A* (2007) 1162(2):154–61. doi:10.1016/j.chroma.2007.05.064

28. Cousins CM, Holownia P, Hawkes JJ, Limaye MS, Price CP, Keay P, et al. Plasma preparation from whole blood using ultrasound. *Ultrasound Med Biol* (2000) 26:881–8. doi:10.1016/s0301-5629(00)00212-x

29. Hawkes J, Coakley WT. Force field particle filter, combining ultrasound standing waves and laminar flow. *Sensors Actuators B: Chem* (2001) 75:213–22. doi:10.1016/s0925-4005(01)00553-6

30. Petersson F, Nilsson A, Jonsson H, Laurell T. Carrier medium exchange through ultrasonic particle switching in microfluidic channels. *Anal Chem* (2005) 77:1216–21. doi:10.1021/ac048394q

31. Haake A, Neild A, Kim D, Ihm J, Sun Y, Dual J, et al. Manipulation of cells using an ultrasonic pressure field. *Ultrasound Med Biol* (2005) 31:857–64. doi:10.1016/j.ultrasmedbio.2005.03.004

32. Neild A, Oberti S, Beyeler F, Dual J, Nelson BJ. A micro-particle positioning technique combining an ultrasonic manipulator and a microgripper. *J Micromech Microeng* (2006) 16:1562–70. doi:10.1088/0960-1317/16/8/017

33. Kapishnikov S, Kantsler V, Steinberg V. Continuous particle size separation and size sorting using ultrasound in a microchannel. *J Stat Mech* (2006) P01012. doi:10.1088/1742-5468/2006/01/p01012

34. Wiklund M, Günther C, Jäger M, Fuhr G, Hertz HM. Ultrasonic standing wave manipulation technology integrated into a dielectrophoretic chip. *Lab Chip* (2006) 6:1537–44. doi:10.1039/b612064b

35. Laurell T, Petersson F, Nilsson A. Chip integrated strategies for acoustic separation and manipulation of cells and particles. *Chem Soc Rev* (2007) 36:492–506. doi:10.1039/b601326k

36. Milne G, Rhodes D, MacDonald M, Dholakia K. Fractionation of polydisperse colloid with acousto-optically generated potential energy landscapes. *Opt Lett* (2007) 32:1144–6. doi:10.1364/ol.32.001144

37. Townsend RJ, Hill M, Harris NR, McDonnell MB. Performance of a quarter-wavelength particle concentrator. *Ultrasonics* (2008) 48:515–20. doi:10.1016/j.ultras.2008.06.005

38. Oberti S, Moeller D, Neild A, Dual J, Beyeler F, Nelson B, et al. Strategies for single particle manipulation using acoustic and flow fields. *Ultrasonics* (2010) 50:247–57. doi:10.1016/j.ultras.2009.09.004

39. Courtney C, Drinkwater OC, Wilcox BW, Demore C, Cochran S, Hill M, et al. Manipulation of microparticles using phase-controllable ultrasonic standing waves. *J Acoust Soc Am* (2010) 128:EL195–9. doi:10.1121/1.3479976

40. Franke T, Braunmuller S, Schmid L, Wixforth A, Weitz DA. Surface acoustic wave actuated cell sorting (SAWACS). *Lab Chip* (2010) 10:789–94. doi:10.1039/b915522h

41. Thalhammer G, Steiger R, Meinschad M, Hill M, Bernet S, Ritsch-Marte M. Combined acoustic and optical trapping. *Biomed Opt Express* (2011) 2:2859. doi:10.1364/boe.2.002859

42. Bazou D, Castro A, Hoyos M. Controlled cell aggregation in a pulsed acoustic field. *Ultrasonics* (2012) 52:842–50. doi:10.1016/j.ultras.2012.01.005

43. Ding X, Lin S-CS, Kraly B, Yue H, Li S, Chiang I-K., et al. On-chip manipulation of single microparticles, cells, and organisms using surface acoustic waves *Proc Nat Acad Sci USA* (2012) 109:11105–9. doi:10.1073/pnas.1209288109

44. Glynne-Jones P, Hill M. Acoustofluidics 23: Acoustic manipulation combined with other force fields. *Lab Chip* (2013) 13:1003–10. doi:10.1039/c3lc41369a

45. González I, Fernandez LJ, Gomez T, Berganzo J, Soto JL, Carrato A. A polymeric chip for micromanipulation and particle sorting by ultrasounds based on a multilayer configuration. *Sensors Actuators B: Chem* (2010) 144:310–7. doi:10.1016/j.snb.2009.10.042

46. González I, Fernandez LJ, Gomez T, Soto JL, Martin A, Berganzo J. Optimizing polymer lab-on-chip platforms for ultrasonic manipulation: Influence of the substrate. *Proc 6th Int Conf Microtechnologies Med Biol* (2011) 6:60–1. doi:10.3390/mi6050574

47. Harris N, Hill M, Keating A, Baylac-Choulet P. A lateral mode flow-through PMMA ultrasonic separator. *Int J Appl Biomed Eng* (2012) 5(8):20–7.

48. Mueller A, Lever A, Nguyen TV, Comolli J, Fiering J. Continuous acoustic separation in a thermoplastic microchannel. *J Micromech Microeng* (2013) 23:125006. doi:10.1088/0960-1317/23/12/125006

49. Hulström J, Manneberg O, Dopf K, Hertz H, Brisma H, Wiklund M. Proliferation and viability of adherent cells manipulated by standing-wave ultrasound in a microfluidic chip. *Ultrasound Med Biol* (2007) 33(1):145–51. doi:10.1016/j.ultrasmedbio.2006.07.024

50. Lenshof A, Ahmad-Tajudin A, Sward AM, Nilsson J, Marko-Varga G. Acoustic whole blood plasmapheresis chip for prostate specific antigen microarray diagnostics. *Anal Chem* (2009) 81:6030–7. doi:10.1021/ac9013572

51. González I, Carreras P, Ahumada O. Ultrasonic enrichment of flowing blood cells in capillars: Influence of the flow rate. *Phys Proced* (2015) 70:72–5. doi:10.1016/j.phpro.2015.08.045

52. Augustsson P, Magnusson C, Nordin M, Lilja H, Laurell T. Microfluidic, label-free enrichment of prostate cancer cells in blood based on acoustophoresis. *Anal Chem* (2012) 84:7954. doi:10.1021/ac301723s

53. González I, Tijero M, Martin A, Acosta V, Berganzo J, Castillejo A, et al. Optimizing polymer lab-on-chip platforms for ultrasonic manipulation: Influence of the substrate. *Micromachines* (2015) 6:574–91. doi:10.3390/mi6050574

54. De los Reyes E, Acosta V, Carreras P, Pinto A, González I. Introduction to the special issue on the theory and applications of acoustofluidics. *J Acoust Soc America* (2021) 150:646. doi:10.1121/10.0009056

55. Muller PB, Rossi M, Marín ÁG, Barnkob R, Augustsson P, Laurell T, et al. Ultrasound-induced acoustophoretic motion of microparticles in three dimensions. *Phys Rev EE* (2013) 88(2):023006. doi:10.1103/physreve.88.023006

56. Barnkob R, Augustsson P, Laurell T, Bruus H. Acoustic radiation- and streaming-induced microparticle velocities determined by microparticle image velocimetry in an ultrasound symmetry plane. *Phys Rev E* (2012) 86:056307. doi:10.1103/physreve.86.056307

57. Kim BP, Meacham JL. Motile cells as probes for characterizing acoustofluidic devices. *Lab Chip* (2021) 21(3):521–33. doi:10.1039/d0lc01025a

58. Kim M, Bayly P, Meacham JL. Motile cells as probes for characterizing acoustofluidic devices. *Lab Chip* (2021) 21(3):521–33. doi:10.1039/D0LC01025A

59. Destgeer G, Jung JH, Ahmed H, Sung HJ. Particle separation inside a sessile droplet with variable contact angle using surface acoustic waves. *Anal Chem* (2017) 89(1):736–44. doi:10.1021/acs.analchem.6b03314

60. Comeau ES, Hocking DC, Dalecki D. Ultrasound patterning technologies for studying vascular morphogenesis in 3D. *J Cel Sci* (2017) 130(1):232–42. doi:10.1242/jcs.188151

61. Gherardini L, Cousins CM, Hawkes JJ, Spengler J, Radel S, Lawler H, et al. A new immobilisation method to arrange particles in a gel matrix by ultrasound standing waves. *Ultrasound Med Biol* (2005) 31(2):261–72. doi:10.1016/j.ultrasmedbio.2004.10.010

62. Laurell T, Lenshof A. *The royal society of chemistry*. Cambridge, UK: Royal society of chemistry (2015). p. 593.

63. Skov NR, Bach JS, Winckelmann BG, Bruus H. 3D modeling of acoustofluidics in a liquid-filled cavity including streaming, viscous boundary layers, surrounding solids, and a piezoelectric transducer. *AIMS Math* (2019) 4(1):99. doi:10.3934/math.2019.1.99

64. Vargas A, Ochoa DC, Delay M, González I, Camacho M. *Ultrasound Med Biol* (2022) 48(7):1202–14. doi:10.1016/j.ultrasmedbio.2022.02.016

65. Townsend R, Hill M, Harris N, White N. Ultrasonics. *Proc Ultrason Int* (2004) 42(1):319–24. doi:10.1016/j.ultras.2008.06.007

66. Koklu M, Sabuncu AC, Beskok A. Acoustophoresis in shallow microchannels. *J Colloid Interf Sci* (2010) 351(2):407–14. doi:10.1016/j.jcis.2010.08.029

67. Gor'kov L. On the forces acting on a small particle in an acoustical field in an ideal fluid. *Sov Phys Acoust* (1962) 6(9):773–5. doi:10.1142/9789814366960_0008

68. Spengler JF, Coakley WT, Christensen KT. Microstreaming effects on particle concentration in an ultrasonic standing wave. *AIChE J* (2003) 49(11):2773–82. doi:10.1002/aic.690491110

69. Bazou D, Kuznetsova LA, Coakley WT. Physical enviroment of 2-D animal cell aggregates formed in a short pathlength ultrasound standing wave trap. *Ultrasound Med Biol* (2005) 31(3):423–30. doi:10.1016/j.ultrasmedbio.2004.12.007

70. Rayyan M, Saint-Martin L, Kamran A. Couplants in acoustic biosensing systems. *Chemosensors* (2022) 10:181. doi:10.3390/chemosensors10050181

71. Poltawski L, Watson T. Relative transmissivity of ultrasound coupling agents commonly used by therapists in the UK. *Ultrasound Med Biol* (2007) 33:120–8. doi:10.1016/j.ultrasmedbio.2006.07.026

72. Ohlin M, Iranmanesh I, Christakou A, Wiklund M. Temperature-controlled MPa-pressure ultrasonic cell manipulation in a microfluidic chip. *Lab Chip* (2015) 15(16):3341–9. doi:10.1039/c5lc00490j

73. Cui M, Kim M, Weisensee PB, Meacham JM. Thermal considerations for microswimmer trap-and-release using standing surface acoustic waves. *Lab Chip* (2021) 21:2534–43. doi:10.1039/d1lc00257k

74. Lei J, Hill M. Glynne-Jones, Numerical simulation of 3D boundary-driven acoustic streaming in microfluidic devices. *Lab Chip* (2014) 14:532–41. doi:10.1039/c3lc50985k